Anomaly Detection using Impedance Measurements on the Boundary

Y. G. Cho[1], O. Kwon[2], J. K. Seo[2], E. J. Woo[3], J. R. Yoon[4]
[1]Graduate School of East-West Medical Sciences, Kyung Hee University, Kyungki, Korea
[2]Department of Mathematics, Yonsei University, Seoul, Korea
[3]School of Electronics and Information, Kyung Hee University, Kyungki, Korea
[4]School of Mathematics, Korea Institute for Advanced Study, Seoul, Korea

Abstract-**We describe a new anomaly detection algorithm based on Electrical Impedance Tomography (EIT) technique. When only the boundary current and voltage measurements are available, it is not practically feasible to reconstruct accurate high-resolution cross-sectional resistivity images of a subject. In this paper, we focus our attention on the detection of the location and size of anomalies with resistivity values different from the background tissues. We show the performance of the algorithm from experimental results using 32-channel EIT system and saline phantoms. The algorithm is applicable to the detection of cancerous tissues in the breast.**
Keywords: **EIT, anomaly, size, location, detection, resistivity**

I. INTRODUCTION

Electrical impedance tomography (EIT) is a medical imaging technique to produce cross-sectional resistivity (or conductivity) images of the human body [1], [2]. Electrodes are placed on the body surface to inject currents and measure voltages. Several image reconstruction algorithms are published to image the spatial distribution of electrical resistivity [2]. Since 1980s, this technique has been received considerable attention in medical imaging area because it may visualize totally new physiological information with many possible clinical applications. In particular, considerable efforts have been devoted to applications in cardiac, respiratory, and breast imaging.

In EIT, we need to find the reconstruction map from the measured boundary data to the cross-sectional resistivity distribution. Unfortunately, unlike the other medical imaging modalities such as x-ray CT and MRI, EIT suffers from the nonlinearity between the measured boundary data and the internal resistivity distribution. Moreover, reconstruction algorithms are severely ill-posed due to the inherent low sensitivity of boundary measurements to any changes of internal tissue resistivity values. This ill-posedness and nonlinearity make EIT not so successful in producing high-resolution images. For the present, with a limited set of measured boundary data, imaging high-quality resistivity distribution seems to be extremely difficult.

In this paper, we focus our attention on the detection instead of imaging. We believe it is more practical to extract only necessary core information by utilizing all available information on the resistivity distribution instead of trying to visualize precise resistivity image extravagantly. For electrical impedance imaging of breast cancer as an example, the resistivity of cancerous tissues differs from that of surrounding normal tissues. In this case, the size and location of the cancerous tissues will be the core information to search for rather than trying to figure out accurate shape of them.

This work was supported by grant No. 2000-2-31400-008-3 from the Basic Research Program of the Korea Science & Engineering Foundation.

We will formulate a model problem of detecting size and location of anomalies such as breast cancer by electrical impedance imaging technique. Our detection algorithm is based on the recent mathematical results that introduced real-time three-dimensional algorithm to detect size and location of anomalies [3], [4]. Here we assume that the differences between resistivity values of anomalies and background are known to be in a fixed range. In this method, the location of anomaly is immediately determined by the pattern of a simple weighted combination of injection currents and measured voltages. We perform several experiments on a saline phantom to demonstrate the accuracy of our detection algorithm.

The experimental results show that our algorithm is quite accurate and stable against measurement noise. The detection process is fast enough to carry out all calculations using an ordinary modern personal computer for real-time monitoring.

II. METHODOLOGY

A. Total Size Detection

We are interested in the inverse problem of finding multiple anomalies, $\cup_{j=1}^{M} D_j$ located in a given conducting body $\Omega \subset \mathbb{R}^n$ (n=2, 3) whose conductivity distribution is of the form,

$$s(x) = 1 + \sum_{j=1}^{M} m c_{D_j} \tag{1}$$

where c_{D_j} is the characteristic function of D_j and m is a positive constant meaning the ratio of conductivity values between the anomalies and background. Then, for a given injection current $g \in L_0^2(\partial\Omega) := \left\{ j \in L^2(\partial\Omega) : \int_{\partial\Omega} j = 0 \right\}$, the electric potential u is governed by the following Neumann problem:

$$\mathfrak{N}[D, g] \begin{cases} \nabla \cdot (s \nabla u) = 0 & \text{in } \Omega \\ \dfrac{\partial u}{\partial n} = g & \text{on } \partial\Omega \text{ and } \int_{\partial\Omega} u\, dl = 0 \end{cases} \tag{2}$$

Report Documentation Page

Report Date	Report Type	Dates Covered (from... to)
25 Oct 2001	N/A	-

Title and Subtitle Anomaly Detection Using Impedance Measurements on the Boundary	**Contract Number**
	Grant Number
	Program Element Number
Author(s)	**Project Number**
	Task Number
	Work Unit Number
Performing Organization Name(s) and Address(es) Graduate School of East-West Medical Sciences Kyung Hee University Kyungki, Korea	**Performing Organization Report Number**
Sponsoring/Monitoring Agency Name(s) and Address(es) US Army Research, Development & Standardization Group (UK) PSC 802 Box 15 FPO AE 09499-1500	**Sponsor/Monitor's Acronym(s)**
	Sponsor/Monitor's Report Number(s)

Distribution/Availability Statement
Approved for public release, distribution unlimited

Supplementary Notes
Papers from 23rd Annual International Conference of the IEEE Engineering in Medicine and Biology Society, October 25-28, 2001, held in Istanbul, Turkey. See also ADM001351 for entire conference on cd-rom., The original document contains color images.

Abstract

Subject Terms

Report Classification unclassified	**Classification of this page** unclassified
Classification of Abstract unclassified	**Limitation of Abstract** UU

Number of Pages
4

where n is the outward unit normal vector on the boundary and dl denotes the surface measure.

In many biomedical applications, it may be very desirable to find the total size using a stable procedure. One important example is the breast cancer detection problem. Now, we describe an algorithm to find the total size of multiple anomalies $\cup_{j=1}^{M} D_j$. Suppose that $\cup_{j=1}^{M} D_j \subset B_R$, which is the ball with radius R centered at $x = 0$ contained in Ω. We choose an injection current $g = \vec{a} \cdot n$ where $\vec{a}$ is a unit constant vector. There exists a unique r_0, $0 < r_0 < R$, so that

$$\int_{\partial\Omega} \left(u - v_{r_0} \right) g \, dl = 0 \tag{3}$$

where u and v_r are solutions of the Neumann problems $\mathfrak{N}[D, g]$ and $\mathfrak{N}[B_r, g]$, respectively. Then, the total size of anomalies $\cup_{j=1}^{M} D_j$ is very close to the size of the ball B_{r_0}.

Various numerical experiments indicate that our algorithm gives a nearly exact estimate for arbitrary multiple anomalies with quite general conductivity values. Its theoretical justification has been studied in [3] where the size estimation has been proved for the case where D is a union of small disks $D_j, j = 1, \ldots, M$ with the following properties;

$$D_j = B_{r_j}\left(z_j \right),\ r_j < e,\ \operatorname{dist}(D_i, D_j) > L \text{ for } i \neq j,\ \operatorname{dist}(D_j, \partial\Omega) > L \tag{4}$$

where L is a fixed positive number and e is a small number. Then, for the unique $r_0 \in (0, R)$ which minimizes the energy [3], the total size of $D = \cup_{j=1}^{M} D_j$ can be approximated by

$$\sum_{j=1}^{M} \left| D_j \right| = \left| B_{r_0} \right| + O(e^4). \tag{5}$$

B. Location Detection

The location search algorithm is based on simple aspects of the function $H(\cdot; g, f)$ in Eq. (6), which is computed directly from the boundary data, that is the applied current g and the measured voltage f.

$$H(x; g, f) := \int_{\partial\Omega} \frac{\partial \Phi(x-y)}{\partial n(y)} f(y) \, ds_y - \int_{\partial\Omega} \Phi(x-y) g(y) \, ds_y \tag{6}$$

where $x \in \mathbb{R}^n \setminus \partial\Omega$ and Φ is the fundamental solution of Laplacian given by

$$\Phi(x-y) := \begin{cases} \dfrac{1}{2p} \log|x-y| & \text{for } n = 2 \\ \dfrac{-1}{4p} \dfrac{1}{|x-y|} & \text{for } n = 3. \end{cases} \tag{7}$$

Integrating by parts and using the transmission boundary condition on ∂D [5], we get

$$H(x; g, f) + m \int_D \nabla_y \Phi(x-y) \cdot \nabla u(y) \, dy = \begin{cases} u(x) \text{ for } x \in \Omega \\ 0 \text{ for } x \in \mathbb{R}^n \setminus \overline{\Omega}. \end{cases} \tag{8}$$

Our problem is now reduced to determine D from the known function $H(x;g,f)$. How to extract the location information from the representation formula in Eq. (8)? In the recent paper [4], we presented the following asymptotic formula for the current flow.

Let Ω be a C^2 domain in $\mathbb{R}^n$ and $g := \vec{a} \cdot n$ be given for a unit vector $\vec{a}$ as a Neumann data for Eq. (2). Suppose $D = \cup_{j=1}^{M} D_j$ satisfies that $D_j = B_{r_j}(z_j)$ with $r_j < e$, $\operatorname{dist}(D_j, D_k) > L$ for $j \neq k$, and $\operatorname{dist}(D_j, \partial\Omega) > L$ for all $j = 1, \ldots, M$ where e and L are fixed positive numbers. Then, the gradient vector field of the solution u in Eq. (2) on D is approximated by

$$\nabla u(x) = \frac{n\vec{a}}{n+m} + O(e^2),\ x \in D \tag{9}$$

By substituting the relation in Eq. (9) to Eq. (8), the formulation in Eq. (8) is reduced to

$$H(x; g, f) = \frac{m}{w_n (n+m)} \int_D \frac{(x-y) \cdot \vec{a}}{|x-y|^n} dy + O(e^4) \tag{10}$$

where w_n denotes the volume of a unit ball in $\mathbb{R}^n$ and $x \in \mathbb{R}^n \setminus \overline{\Omega}$.

We can find a key information on the location of D from observations of the function $H(\cdot; g, f)$ on $\mathbb{R}^n \setminus \partial\Omega$. If we assume that $\Omega = B_1 \subset \mathbb{R}^2$ and $D := B_r(z)$ is a small ball centered at z with radius r in Ω, the mean value theorem for harmonic functions applied to Eq. (10) yields

$$H(x; g, f) = \frac{mr^2}{2+m} \frac{(x-z) \cdot \vec{a}}{|x-z|^2} + O(e^4),\ x \in \mathbb{R}^2 \setminus \overline{\Omega}. \tag{11}$$

Applying the injection current $g = (0,1) \cdot n$ and taking two observation regions of $\Sigma_1 = \left\{ x = (2, x_2) \in \mathbb{R}^2 \setminus \overline{\Omega} \right\}$ and $\Sigma_2 = \left\{ x = (x_1, -2) \in \mathbb{R}^2 \setminus \overline{\Omega} \right\}$, we can derive the following equation,

$$H(x; g, f) \approx \begin{cases} \dfrac{mr^2}{2+m} \dfrac{x_2 - z_2}{(2 - z_1)^2 + (x_2 - z_2)^2} & \text{if } x \in \Sigma_1 \\ \dfrac{mr^2}{2+m} \dfrac{-2 - z_2}{(x_1 - z_1)^2 + (2 + z_2)^2} & \text{if } x \in \Sigma_2. \end{cases} \tag{12}$$

Therefore, by taking a zero point of $H(x;g,f)$ on Σ_1 and a critical point of $H(x;g,f)$ on Σ_2, we can determine the location of D. Fig. 1 illustrates the relation between the location of D and the observation function $H(x;g,f)$ on Σ_1 and Σ_2.

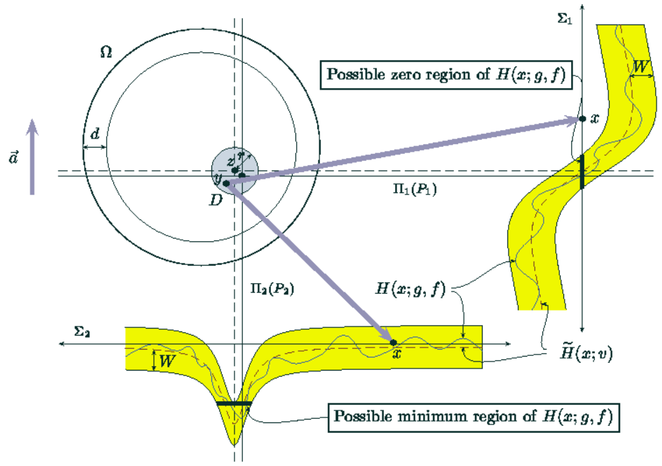

Fig. 1. Location of an anomaly and the pattern of $H(x;g,f)$ for $m > 0$

III. RESULTS

A. EIT Hardware and Phantom

We present experimental results in detecting the location and size of anomalies in a circular saline phantom with 32 electrodes attached on the boundary with equal distance between them. Fig. 2 shows the phantom and 32-channel EIT system. The EIT system provides a way to inject different patterns of currents and measure voltages on the electrodes. It, therefore, includes 32 independent current sources whose output is 50 kHz sinusoid with variable amplitude. The EIT system is interfaced to a PC and a control program sets the amount of injection current for each current source.

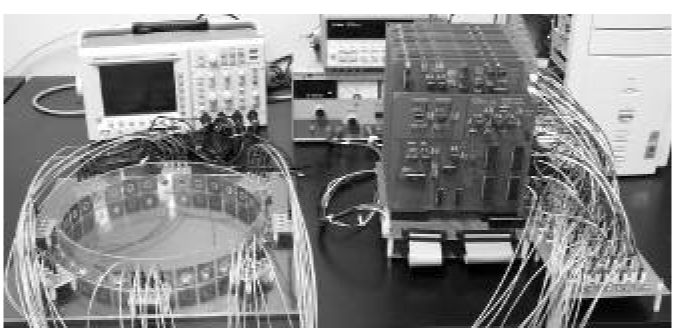

Fig. 2. EIT hardware and phantom

While we inject a pattern of currents through all 32 electrodes, boundary voltage on each electrode is sequentially measured. Voltage measuring circuits consist of a narrow-band variable-gain ac amplifier, a phase-sensitive demodulator, and a 12-bit A/D converter.

We fill the phantom with electrolyte solution of known conductivity value. Anomalies with different conductivity values and shapes are placed inside the phantom. For numerical experiments, the circular phantom is normalized to a unit disc Ω in $\mathbb{R}^2$ and apply the injection current pattern (Neumann data); $g = (0,1)\cdot n(\Gamma_j)$ where Γ_j denotes electrodes, $j = 0, \ldots, 31$.

B. Experimental Results

Unavoidable noise comes from various sources; the circular phantom is not exactly a disc, the electrodes are not exactly equally spaced, and there exist errors in the amount of injection currents and measured voltage data. In order to find the accuracy of our EIT system, we define the relative error as

$$E := \frac{\max_j \left| f(z_j) - f_m(\Gamma_j) \right|}{\max_j \left| g(\Gamma_j) \right|} \qquad (13)$$

where f is the analytically computed boundary voltage, f_m is the measured boundary voltage, and g is the injection current. We set the magnitude of injection current at each electrode as sin(jq) where j is the electrode number from 0 to 31 and q is the angle between adjacent two electrodes. For this kind of injection current pattern, measured voltages on each electrode should have the same sin(jq) pattern and the relative error was 4.6%.

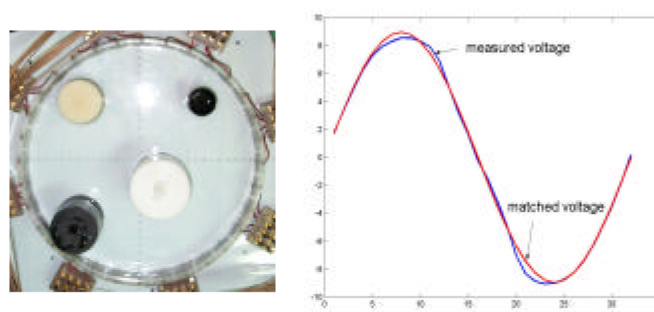

(a) Target (b) Boundary Measurements

Fig. 3. Experimental result of the total size detection

We put four anomalies in the phantom with 290mm diameter as shown in Fig. 3. Using boundary voltage measurements, the total size of four anomalies (diameter of the equivalent ball) was computed as 131.6mm. Since the true total size is 125.0mm, the error in size detection is about 5.3%.

In Fig. 4, we put one anomaly in the phantom. Using the boundary voltage measurements for the injection current pattern of sin(*jq*), we found the location of the anomaly as shown in Fig. 4(c).

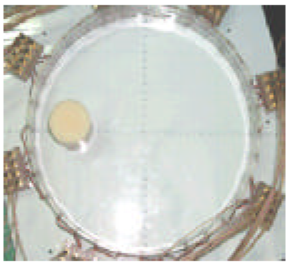

(a) Target

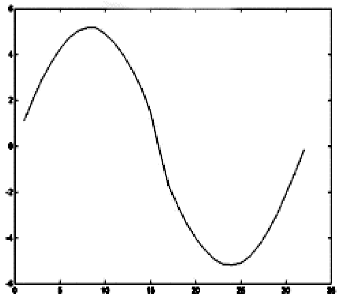

(b) Boundary Measurements

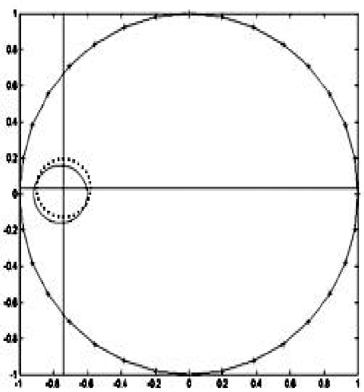

(c) Location detection

Fig. 4. Experimental result of the location detection

IV. Discussion

Since the detection accuracy is dependent on the measurement accuracy, we need to improve the performance of our EIT system. We found that the accuracy in the detected size is not dependent on the location of anomaly. This means that the detection of a small anomaly at the center is not particularly more difficult than the detection of the same anomaly at the periphery. When there are multiple anomalies, current algorithm finds the total size and the location in terms of the center of conductivity values.

Future study should include the individual detection of multiple anomalies. We may use the algorithm described in this paper to find the total size and the location. Then, we can use this information as an initial guess for an iterative resistivity image reconstruction algorithm. During image reconstruction, we can also use this information as a constraint on the reconstructed resistivity image.

V. Conclusion

We developed a new anomaly detection algorithm using an EIT system. Assuming that we measure the boundary current and voltage data on the surface electrodes, the detection algorithm finds the location of an anomaly when the resistivity of the anomaly is different from that of the background. It also produces the total area of multiple anomalies.

When there are multiple anomalies, it finds the location of the anomalies in terms of the center of resistivity values. We plan to develop a new EIT system with an improved accuracy and an electrode interface unit for applying electrodes on the breast. This kind of breast cancer detection system will be a good alternative to x-ray mammography for patient screening purpose.

References

[1] J. G. Webster, ed., *Electrical Impedance Tomography*, Bristol, UK, Adam Hilger, 1990.

[2] K. Boone, D. Barber, and B. Brown, "Imaging with electricity: report of the European concerted action on impedance tomography," *J. Med. Eng. Tech.*, vol. 21, no. 6, pp. 201-232, 1997.

[3] O. Kwon and J. K. Seo, "Total size estimation and identification of multiple anomalies in the inverse electrical impedance tomography," *Inverse Problems*, vol. 17, pp. 59-75, 2001.

[4] O. Kwon, J. K. Seo, and J. R. Yoon, "A real time algorithm for the location search of discontinuous conductivities with one measurement," submitted for publication.

[5] H. Kang and J. K. Seo, "Layer potential technique for the inverse conductivity problem," *Inverse Problems*, vol. 12, pp. 267-278, 1996.